# Chapter 3
# Appraisal of Land Use/Land Cover Change Over Tehri Catchment Using Remote Sensing and GIS

**Sabyasachi Swain, Surendra Kumar Mishra, and Ashish Pandey**

**Abstract** The Himalayan reservoirs have immense significance from the point of view of water resources planning and management. However, natural and anthropogenic changes and their effects upon these reservoirs are often not explored, mainly due to limitations of data availability. This chapter presents an appraisal of land use/land cover (LULC) changes over the Tehri catchment located at the lower Himalayan region, using remote sensing and geographic information system (GIS). The imageries are collected for different years, i.e., 2008, 2014, and 2020 from the Landsat 5, Landsat 8, and Sentinel 2 satellites, respectively, with the objective of deriving information on different LULC classes. Following a supervised classification, the catchment area is divided into eight classes, viz. open forest, dense forest, water bodies, shrubland, agricultural land, settlements, barren land, and snow covers. The accuracy of classification is assessed with respect to the Google Earth images and ground truth verification. A comparison between the areal coverage of the LULC classes was analyzed for temporal LULC change detection over the catchment. Comparing 2008 and 2020, it is clear that the dense forests and barren land have decreased. On the other hand, an increase in the open forests, water bodies, shrubland, snow, and settlement is observed. The accuracy assessment results confirm that the LULC changes reported in this study are justifiably accurate and utilizable for further applications. The results reported in this study may be helpful to frame solutions to hydrological problems of the Tehri catchment. Moreover, this study highlights the usefulness of remote sensing and GIS in hydrological applications, even in mountainous catchments.

---

S. Swain (✉) · S. K. Mishra · A. Pandey
Department of Water Resources Development and Management, Indian Institute of Technology Roorkee, Roorkee, Uttarakhand 247 667, India
e-mail: sswain@wr.iitr.ac.in

S. K. Mishra
e-mail: s.mishra@wr.iitr.ac.in

A. Pandey
e-mail: ashish.pandey@wr.iitr.ac.in



A. Pandey et al. (eds.), *Geospatial Technologies for Land and Water Resources Management*, Water Science and Technology Library 103,
https://doi.org/10.1007/978-3-030-90479-1_3

## 3.1 Introduction

In India, the continuous demand for economic growth coupled with the population explosion has resulted in substantial land use/land cover (LULC) changes in the past century (Tian et al. 2014). The ramifications of LULC changes include influencing ecosystem services, altering hydrological components, triggering and intensifying the natural hazards, complicating the hydroclimatic predictions, affecting quantity and quality of available water resources, etc. (Aadhar et al. 2019; Astuti et al. 2019; Bahita et al. 2021; Chen et al. 2020; Hengade and Eldho 2016; Saputra and Lee 2019; Sharma et al. 2020; Singh et al. 2020; Swain et al. 2018, 2019a, b; Talukdar et al. 2020; Tripathi et al. 2020). The impacts of droughts are more severe, where the LULC is mostly dedicated to agriculture (Swain et al. 2017, 2020a, 2021a, b, b). An improved understanding of the LULC and climatic changes of a particular area can be pivotal for effective policy framing, specifically in water resources planning and management (Anand et al. 2018; Himanshu et al. 2018, 2019; Dayal et al. 2019, 2021; Guptha et al. 2021; Kalura et al. 2021; Sahoo et al. 2021). Due to all these reasons, a detailed assessment of LULC change patterns has become necessary, which is typically carried out by analyzing historical LULC changes through multi-temporal remotely sensed images. Several research works have been carried out in the last few years to investigate the LULC changes, their future predictions, and consequential effects (Dutta et al. 2019; Liping et al. 2018; Palmate et al. 2017a, b; Pandey and Khare 2017; Pandey and Palmate 2018; Rimal et al. 2017; Rwanga and Ndambuki 2017; Singh et al. 2018; Tran et al. 2017).

The Himalayan catchments have immense significance from the point of view of water resources planning and management (Singh and Pandey 2021; Swain et al. 2021c). However, the natural and anthropogenic changes and their effects upon these reservoirs are often not explored, mainly due to limitations of data availability. With the advancement of remote sensing and geospatial technologies, the LULC information of these catchments have become easily accessible. Recently, Mishra et al. (2020) used Landsat 5 and Sentinel 2A for supervised LULC classification over the Rani Khola watershed located in the Sikkim Himalaya, India. They reported a series of complicated changes in LULC over the watershed during 1988–2017. Therefore, this study aims to carry out a detailed assessment of LULC changes over a Himalayan catchment considering multi-temporal satellite images and supervised classification. Further, it is wise to cross-check the LULC classification of the recent period by ground truth verification. In this regard, the details of the study area, methodology, results and discussion, ground-truthing information, and the conclusions derived from this study are presented in the subsequent sections.

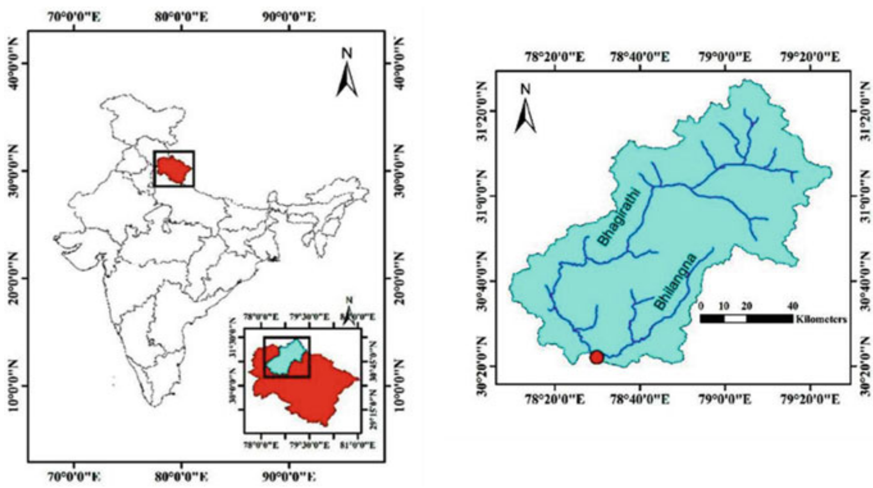


**Fig. 3.1** Location map of the study area

## 3.2 Study Area and Data

The Tehri catchment located in the state of Uttarakhand, India, is considered as the study area. The catchment covers an area of 7295 km$^2$. The catchment lies in the lower Himalayan region and thus is associated with very steep slopes. This is the main reason for the very high velocity of flow, which consequently leads to mass erosion. The location of the study area is shown in Fig. 3.1. The maximum and minimum temperatures over the catchment are 36 °C in summer and 0 °C in winter, respectively. A good amount of rainfall is received all over the catchment, though there are remarkable spatial variations (Kumar and Anbalagan 2015; Rautela et al. 2002).

The satellite-based imageries were collected from the website of United States Geological Survey (USGS) EarthExplorer. While the image for 2008 was taken from Landsat 5, the images for 2014 and 2020 were taken from Landsat 8 and Sentinel 2 satellites, respectively.

## 3.3 Methodology

The extraction of LULC information from the imageries is carried out by remote sensing and GIS techniques. The two softwares, viz. ERDAS IMAGINE and ArcGIS are widely used to carry out different image processing and geospatial operations, which were also used in this study. The overall methodology adopted for LULC classification and change detection is presented in Fig. 3.2. First of all, the satellite images for different years are collected and their preprocessing is carried out. The area of

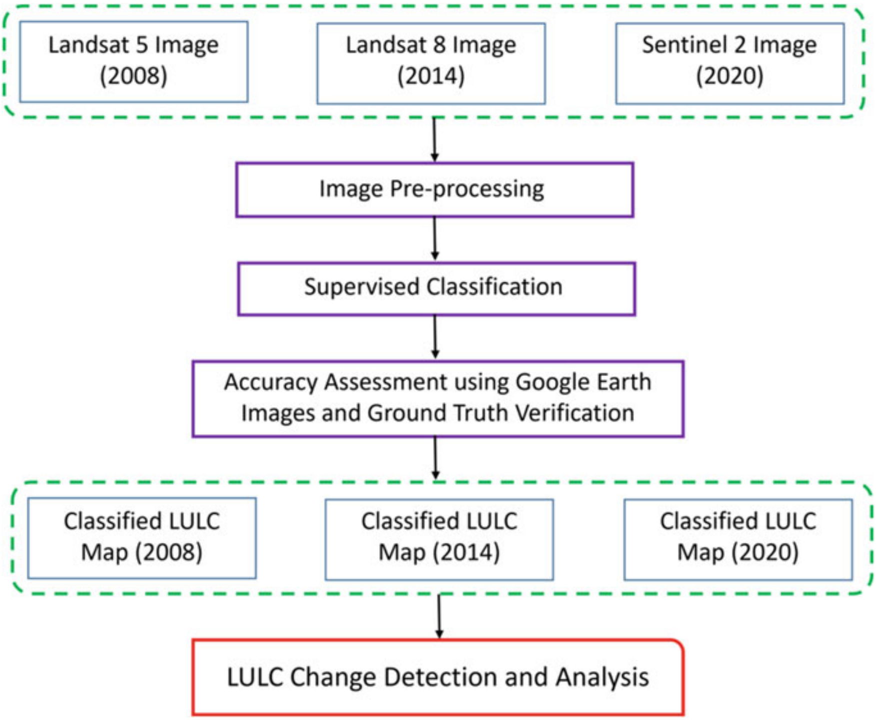


**Fig. 3.2** Overall methodology for analyzing the multi-temporal LULC changes

interest may not fall under a single satellite image, and the collected data may be available in different file formats or projection systems. Therefore, stacking, mosaicing, and adjusting the coordinate systems, etc., were performed using ERDAS IMAGINE and ArcGIS 10.2.4 softwares. Moreover, for better interpretation of the imageries, false-color composites, contrast stretching, and image enhancement operations were also carried out.

The next step is the supervised classification, where the sample pixels in an image representing particular classes are selected by the user based on his/her knowledge. These are called the input classes or the training sites. The classification of all the remaining pixels can be carried out using these training sites through an image processing software. The reflectance of each pixel is the core of the image classification. For a particular class, the higher the number of training sites, the better is the precision of the classification. Therefore, LULC classification is based on the concept of segmenting the spectral domain into distinct ground cover classes. In this study, the study area is divided into eight different LULC classes, viz. open forest, dense forest, water bodies, shrubland, agricultural land, settlements, barren land, and snow covers.

The next step is the accuracy assessment, whose purpose is to validate the classification results. This justifies the utility of the classified maps for further applications.

**Table 3.1** Measures for accuracy assessment of classification

| Accuracy measures | Formula |
|---|---|
| Producer accuracy ($A_P$) | $\frac{x_{ij}}{x_j}$ |
| User accuracy ($A_U$) | $\frac{x_{ij}}{x_i}$ |
| Overall accuracy ($A_O$) | $\frac{1}{N}\sum_{i=j=1}^{n} x_{ij}$ |
| Kappa coefficient ($K_C$) | $\frac{N\times\sum_{i=j=1}^{n} x_{ij}-\sum_{i=j=1}^{n}(x_i\times x_j)}{N^2-\sum_{i=j=1}^{n}(x_i\times x_j)}$ |

$x_{ij}$ = value of $i$th row and $j$th column, $x_j$ = sum of all values in $j$th column, $x_i$ = sum of all values in $i$th row, $N$ = total number of reference points, $n$ = total number of rows/columns

This can be achieved by ground truth verification in terms of field visits. However, it is practically infeasible to collect information on the entire study area through field visits. Moreover, ground-truthing of the LULC for past years is almost impossible. Therefore, Google Earth images for a particular period can be used as a reference for validating the classifications. Using Google Earth as the reference is convenient and requires minimal cost. Nevertheless, for assessing the classification accuracy relevant to the recent period, it is always wise to conduct a field visit to some portions of the study area.

In this study, 400 random points from various classes were taken across the LULC maps. Considering their corresponding points from Google Earth image or ground-truthing information, a confusion matric is prepared. The producer accuracy ($A_P$) and the user accuracy ($A_U$) are calculated for each LULC class, whereas the overall classification accuracy ($A_O$) and the Kappa coefficient ($K_C$) are calculated to assess the LULC classification of the entire area. $A_P$, $A_U$, and $A_O$ are expressed in percentage with a range from 0 to 100. On the other hand, $K_C$ ranges from 0 to 1. The formula for these accuracy measures is provided in Table 3.1. The detailed procedure of accuracy assessment may be referred from literature (Manandhar et al. 2009; Rwanga and Ndambuki 2017; Sarkar 2018). Following the accuracy assessment, the spatiotemporal LULC changes are detected and analyzed.

## 3.4 Results and Discussion

The multi-temporal remotely sensed imageries were used for the detailed LULC classification. The classified maps of the years for 2008, 2014, and 2020 are presented in Fig. 3.3. The spatial variation of LULC classes (open forest, dense forest, water bodies, shrubland, agricultural land, settlements, barren land, and snow covers) in different years can be visualized clearly.

The areal coverage details of the individual classes in 2008, 2014, and 2020 are presented in Table 3.2. For all three years, it can be observed that the dense forest is the most dominant LULC class over the catchment, followed by shrubland and barren land. A significant portion of the catchment is covered by snow, which is

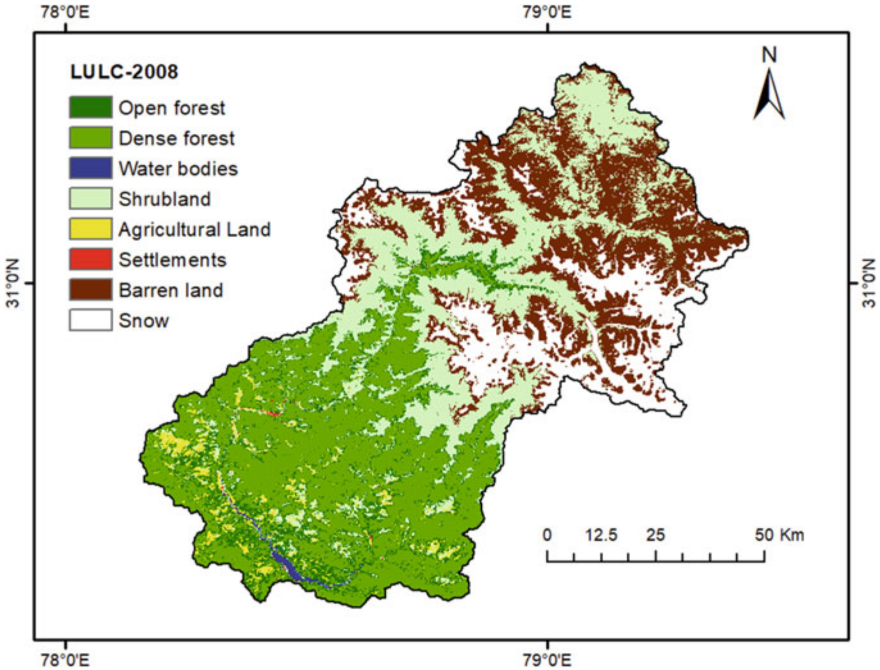


(a) Classified LULC map for 2008

**Fig. 3.3** Multi-temporal supervised classification of LULC over Tehri catchment

inherent in the Himalayan conditions. The settlement constitutes the least portions of the catchment among all the classes.

From Table 3.2, the temporal changes in individual LULC classes over the Tehri catchment can be noticed. The percentage of catchment area under each of these classes during 2008, 2014, and 2020 is also presented. The dense forest has decreased by nearly 60 km$^2$ from 2008 to 2014, whereas there is no change between 2014 and 2020. On the other hand, there is a clear increase in open forests from 2008 to 2014. Hence, it can be fairly inferred that the canopy density has reduced over the years. As a result, the dense forests have been converted to open forests. An increase in the settlement is also observed. These may be attributed to anthropogenic activities, resulting in aggravated soil erosion. No appreciable change in agricultural land is observed between 2008, 2014, and 2020. There is a decrease in barren lands over the years. The shrubland has witnessed a remarkable increase from 2008 to 2014. Similarly, there is a clear increase in the snow covers from 2014 to 2020. The LULC changes were drastic from 2008 to 2014 over most of the classes, whereas there is hardly any change in LULC classes from 2014 to 2020, excluding barren land and snow (Table 3.2).

The results of the accuracy assessment are presented in Table 3.3. Considering the Google Earth images and the information collected during the field visits, the

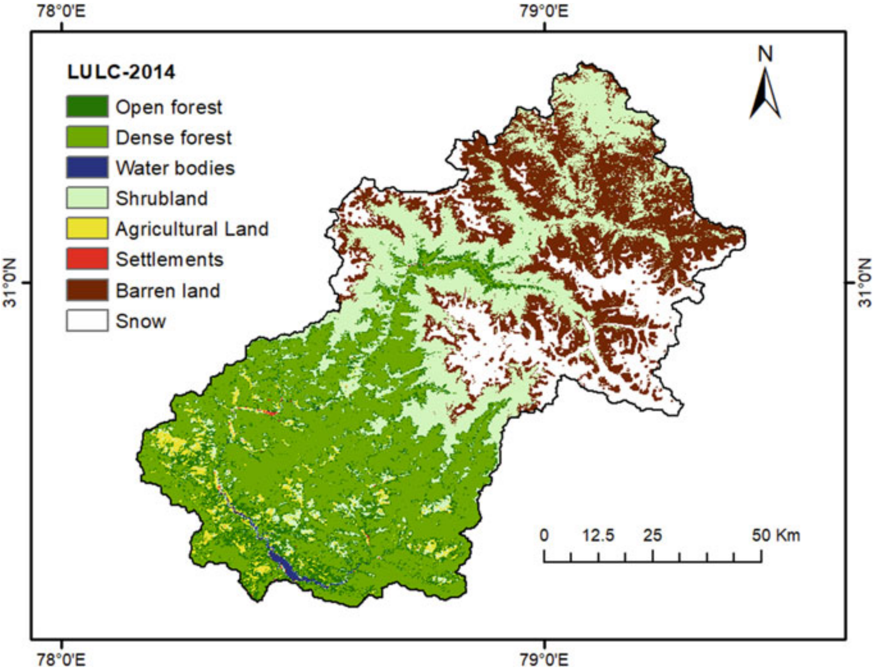


(b) Classified LULC map for 2014

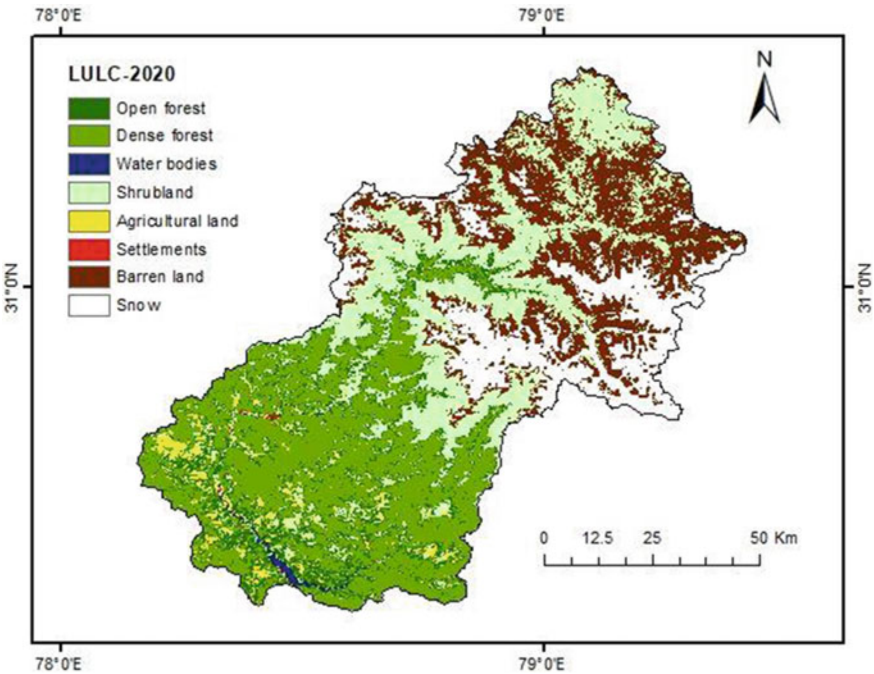


(c) Classified LULC map for 2020

**Fig. 3.3** (continued)

**Table 3.2** Areal coverage details of LULC classes over the Tehri catchment

| Sl. No. | LULC class | 2008 | | 2014 | | 2020 | |
|---|---|---|---|---|---|---|---|
| | | Area (km$^2$) | % Area | Area (km$^2$) | % Area | Area (km$^2$) | % Area |
| 1 | Open forest | 648.5 | 8.89 | 713.5 | 9.78 | 712.7 | 9.77 |
| 2 | Dense forest | 2197.3 | 30.12 | 2140.4 | 29.34 | 2139.6 | 29.33 |
| 3 | Water bodies | 23.3 | 0.32 | 27.0 | 0.37 | 35.0 | 0.48 |
| 4 | Shrubland | 1691.7 | 23.19 | 1780.0 | 24.4 | 1773.4 | 24.31 |
| 5 | Agricultural land | 176.5 | 2.42 | 172.9 | 2.37 | 171.4 | 2.35 |
| 6 | Settlement | 4.4 | 0.06 | 5.1 | 0.07 | 5.8 | 0.08 |
| 7 | Barren land | 1591.0 | 21.81 | 1486.7 | 20.38 | 1434.2 | 19.66 |
| 8 | Snow | 962.2 | 13.19 | 968.8 | 13.28 | 1022.0 | 14.01 |
| Total | | 7295 | 100 | 7295 | 100 | 7295 | 100 |

**Table 3.3** Accuracy assessment results of LULC classification

| LULC class | Accuracy (%) | 2008 | 2014 | 2020 |
|---|---|---|---|---|
| Open forest | Producer | 88.2 | 85.3 | 94.4 |
| | User | 84.0 | 88.9 | 90.9 |
| Dense Forest | Producer | 95.7 | 87.3 | 96.0 |
| | User | 94.2 | 89.2 | 92.5 |
| Water Bodies | Producer | 100.0 | 97.9 | 100.0 |
| | User | 100.0 | 96.0 | 97.4 |
| Shrubland | Producer | 86.3 | 81.7 | 85.0 |
| | User | 80.0 | 83.3 | 86.4 |
| Agricultural Land | Producer | 85.0 | 78.3 | 92.0 |
| | User | 86.7 | 82.0 | 90.0 |
| Settlement | Producer | 84.0 | 82.4 | 91.7 |
| | User | 84.0 | 87.5 | 93.3 |
| Barrenland | Producer | 73.3 | 78.8 | 80.0 |
| | User | 78.0 | 74.5 | 86.0 |
| Snow | Producer | 82.2 | 83.7 | 86.2 |
| | User | 79.2 | 80.0 | 84.0 |
| Overall classification accuracy (%) | | 83.6 | 82.5 | 88.9 |
| Kappa coefficient | | 0.821 | 0.803 | 0.873 |

accuracy measures were estimated. The $A_P$ and $A_U$ values for individual classes are quite encouraging (Table 3.3). The results of the accuracy assessment reflect a precise identification of LULC classes over the catchment for all three periods. The overall classification accuracy (Kappa coefficient) for 2008, 2014, and 2020 are found to be 83.6 (0.821), 82.5 (0.803), and 88.9 (0.873), respectively. These high values of $A_O$ and $K_C$ confirm that the LULC changes reported in this study can be justifiably regarded as accurate and, hence, are utilizable for further applications.

## 3.5 Ground Truth Verification

It is always wise to cross-check the supervised detailed LULC classification by ground truth verification. Therefore, a field visit was made to some portions of the catchment area to collect the land use/land cover observations along with their appropriate location details so that it would be helpful for proper validation and accuracy assessment. Moreover, it aimed to obtain relevant information from the local people regarding the causes of LULC changes, other hydrological problems over the study area (particularly soil erosion), and steps taken to combat those issues. This can be very helpful in preparing an effective catchment area treatment plan. Thus, a field visit was made to accomplish the aforementioned objectives. The details of the locations are provided in Fig. 3.4 and Table 3.4.

Due to the constraints of cost and time, only a portion of the catchment was covered during the field visit. The photographs collected during the field visits along with their location details were useful for the accuracy assessment of the LULC classification pertaining to 2020. A few photographs are presented in Fig. 3.5. As the catchment is prone to soil erosion, several protection measures were adopted, which is evident from some of the photographs (Fig. 3.5).

## 3.6 Conclusion

The detailed supervised LULC classification for the Tehri catchment is carried out using the Landsat 5, Landsat 8, and Sentinel 2 data pertaining to 2008, 2014, and 2020, respectively. The various land covers that the catchment area is classified into are water bodies, agricultural land, dense forest, open forest, shrubland, settlement, barren land, and snow. The LULC changes are found to be drastic from 2008 to 2014 over most of the classes, whereas no appreciable changes in classes are found from 2014 to 2020 except for snow and barren lands. Comparing 2008 and 2020, an increase in the open forests, water bodies, shrubland, snow, and settlement is observed, whereas a decrease in dense forests and barren land is noticed. The accuracy assessment results confirm that the LULC changes reported in this study are justifiably accurate and utilizable for further applications.

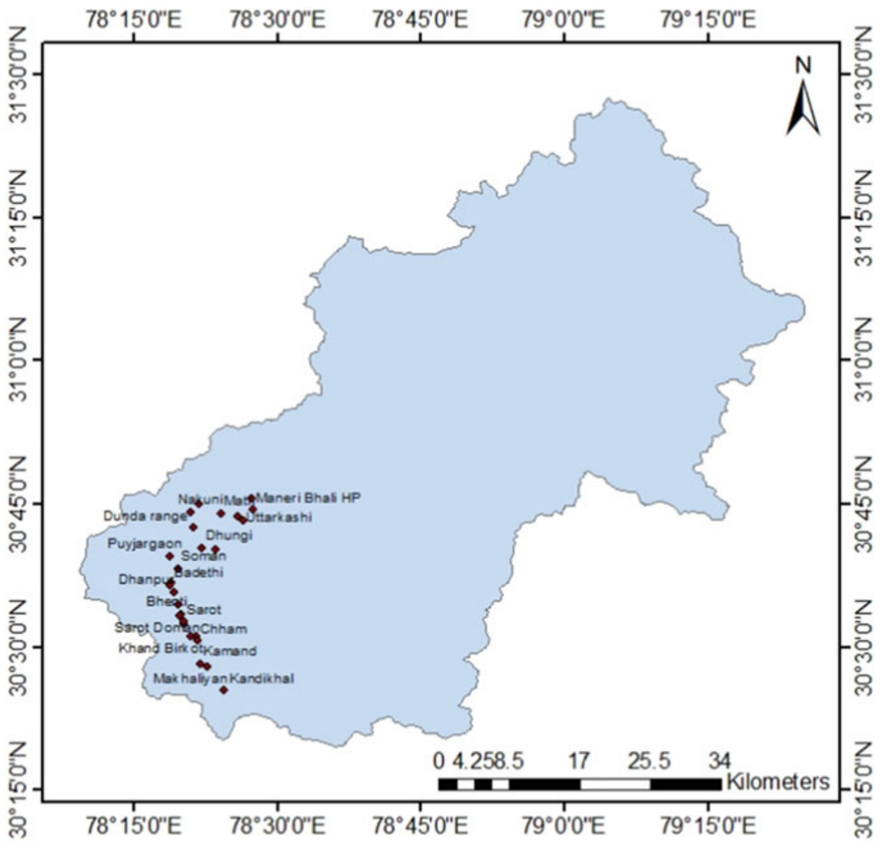


**Fig. 3.4** Locations covered during the field visit

**Table 3.4** Location details of the points covered during the field visit

| S. No. | Name | Latitude (°N) | Longitude (°E) |
|---|---|---|---|
| 1 | Kandikhal | 30.424 | 78.408 |
| 2 | Makhaliyan | 30.466 | 78.378 |
| 3 | Kamand | 30.471 | 78.365 |
| 4 | Chham | 30.511 | 78.360 |
| 5 | Khand Birkot | 30.518 | 78.349 |
| 6 | Manjaruwal Village | 30.519 | 78.359 |
| 7 | Unial Village | 30.540 | 78.336 |
| 8 | Sarot | 30.545 | 78.337 |
| 9 | Sarot Doman | 30.554 | 78.329 |
| 10 | Bhenti | 30.558 | 78.332 |
| 11 | Chinyalisaur | 30.574 | 78.328 |
| 12 | Dhanpur | 30.597 | 78.319 |
| 13 | Badethi | 30.608 | 78.314 |
| 14 | Pujar Village | 30.611 | 78.315 |
| 15 | Dharashu Band | 30.613 | 78.316 |
| 16 | Soman | 30.637 | 78.327 |
| 17 | Puyjargaon | 30.659 | 78.314 |
| 18 | Singuni | 30.671 | 78.392 |
| 19 | Dhungi | 30.674 | 78.369 |
| 20 | Dunda range | 30.709 | 78.353 |
| 21 | Uttarkashi | 30.721 | 78.440 |
| 22 | Maneri Bhali | 30.730 | 78.431 |
| 23 | Matli | 30.734 | 78.401 |
| 24 | Nakuni | 30.737 | 78.350 |
| 25 | Maneri Bhali HP | 30.740 | 78.458 |
| 26 | Genwala | 30.751 | 78.364 |
| 27 | Assi Ganga Sangam | 30.760 | 78.456 |

Terrace Farming (Makhaliyan)

Assi Ganga Sangam

Erosion control measures (Near Matli)

Flood protection measures (Unial Gaon)

Dense Forests (Varunavat Mountain, Uttarkashi)

Degraded Forest (Near Maneri Bhali HP)

**Fig. 3.5** Photographs of some locations in the Tehri catchment collected during the field visit

**Acknowledgements** This study is a part of the project THD-1176-WRC sponsored by the Tehri Hydro Development Corporation India Limited (THDCIL). The authors are thankful to THDCIL for the same. The resources and facilities provided by the Department of Water Resources Development and Management (WRD&M), IIT Roorkee, are acknowledged. The support provided by Lingaraj Dhal and Praveen Kalura during the study is also thankfully acknowledged.

## References

Aadhar S, Swain S, Rath DR (2019) Application and performance assessment of SWAT hydrological model over Kharun river basin, Chhattisgarh, India. In: World Environmental and Water Resources Congress 2019: watershed management, irrigation and drainage, and water resources planning and management. American Society of Civil Engineers, pp 272–280

Anand J, Gosain AK, Khosa R (2018) Prediction of land use changes based on land change modeler and attribution of changes in the water balance of ganga basin to land use change using the SWAT model. Sci Total Environ 644:503–519

Astuti IS, Sahoo K, Milewski A, Mishra DR (2019) Impact of land use land cover (LULC) change on surface runoff in an increasingly urbanized tropical watershed. Water Resour Manage 33(12):4087–4103

Bahita TA, Swain S, Dayal D, Jha PK, Pandey A (2021) Water quality assessment of upper ganga canal for human drinking. In: Climate impacts on water resources in India. Springer, Cham, pp 371–392

Chen Q, Chen H, Zhang J, Hou Y, Shen M, Chen J, Xu C (2020) Impacts of climate change and LULC change on runoff in the Jinsha River Basin. J Geog Sci 30(1):85–102

Dayal D, Gupta PK, Pandey A (2021) Streamflow estimation using satellite-retrieved water fluxes and machine learning technique over monsoon-dominated catchments of India. Hydrol Sci J 66(4):656–671

Dayal D, Swain S, Gautam AK, Palmate SS, Pandey A, Mishra SK (2019) Development of ARIMA model for monthly rainfall forecasting over an Indian River Basin. In: World Environmental and Water Resources Congress 2019: watershed management, irrigation and drainage, and water resources planning and management. American Society of Civil Engineers, pp 264–271

Dutta D, Rahman A, Paul SK, Kundu A (2019) Changing pattern of urban landscape and its effect on land surface temperature in and around Delhi. Environ Monit Assess 191(9):1–15

Guptha GC, Swain S, Al-Ansari N, Taloor AK, Dayal D (2021) Evaluation of an urban drainage system and its resilience using remote sensing and GIS. Remote Sens Appl: Soc Environ 23100601. https://doi.org/10.1016/j.rsase.2021.100601

Hengade N, Eldho TI (2016) Assessment of LULC and climate change on the hydrology of Ashti Catchment, India using VIC model. J Earth Syst Sci 125(8):1623–1634

Himanshu SK, Pandey A, Patil A (2018) Hydrologic evaluation of the TMPA-3B42V7 precipitation data set over an agricultural watershed using the SWAT model. J Hydrol Eng 23(4):05018003. https://doi.org/10.1061/(ASCE)HE.1943-5584.0001629

Himanshu SK, Pandey A, Yadav B, Gupta A (2019) Evaluation of best management practices for sediment and nutrient loss control using SWAT model. Soil Tillage Res 19242–19258. https://doi.org/10.1016/j.still.2019.04.016

Kalura P, Pandey A, Chowdary VM, Raju PV (2021) Assessment of hydrological drought vulnerability using geospatial techniques in the Tons River Basin India. J Ind Soc Rem Sens. https://doi.org/10.1007/s12524-021-01413-7

Kumar R, Anbalagan R (2015) Landslide susceptibility zonation in part of Tehri reservoir region using frequency ratio, fuzzy logic and GIS. J Earth Syst Sci 124(2):431–448

Liping C, Yujun S, Saeed S (2018) Monitoring and predicting land use and land cover changes using remote sensing and GIS techniques—a case study of a hilly area, Jiangle, China. PloS One 13(7)

Manandhar R, Odeh IO, Ancev T (2009) Improving the accuracy of land use and land cover classification of Landsat data using post-classification enhancement. Remote Sens 1(3):330–344

Mishra PK, Rai A, Rai SC (2020) Land use and land cover change detection using geospatial techniques in the Sikkim Himalaya, India. Egypt J Remote Sens Space Sci 23(2):133–143

Palmate SS, Pandey A, Mishra SK (2017) Modelling spatiotemporal land dynamics for a trans-boundary river basin using integrated cellular automata and Markov Chain approach. Appl Geogr 82:11–23

Palmate SS, Pandey A, Kumar D, Pandey RP, Mishra SK (2017) Climate change impact on forest cover and vegetation in Betwa Basin, India. Appl Water Sci 7(1):103–114

Pandey A, Palmate SS (2018) Assessments of spatial land cover dynamic hotspots employing MODIS time-series datasets in the Ken River Basin of Central India. Arab J Geosci 11(17):1–8

Pandey BK, Khare D (2017) Analyzing and modeling of a large river basin dynamics applying integrated cellular automata and Markov model. Environ Earth Sci 76(22):1–12

Rautela P, Rakshit R, Jha VK, Gupta RK, Munshi A (2002) GIS and remote sensing-based study of the reservoir-induced land-use/land-cover changes in the catchment of Tehri dam in Garhwal Himalaya, Uttaranchal (India). Curr Sci 308–311

Rimal B, Zhang L, Keshtkar H, Wang N, Lin Y (2017) Monitoring and modeling of spatiotemporal urban expansion and land-use/land-cover change using integrated Markov chain cellular automata model. ISPRS Int J Geo Inf 6(9):288

Rwanga SS, Ndambuki JM (2017) Accuracy assessment of land use/land cover classification using remote sensing and GIS. Int J Geosci 8(04):611

Sahoo S, Swain S, Goswami A, Sharma R, Pateriya B (2021) Assessment of trends and multi-decadal changes in groundwater level in parts of the Malwa region Punjab India. Groundwater Sustain Dev 14100644. https://doi.org/10.1016/j.gsd.2021.100644

Saputra MH, Lee HS (2019) Prediction of land use and land cover changes for north Sumatra, Indonesia, using an artificial-neural-network-based cellular automaton. Sustainability 11(11):3024

Sarkar A (2018) Accuracy assessment and analysis of land use land cover change using geoinformatics technique in Raniganj Coalfield Area, India. Int J Environ Sci Nat Resour 11(1):25–34

Sharma I, Mishra SK, Pandey A, Kumre SK, Swain S (2020) Determination and verification of antecedent soil moisture using soil conservation service curve number method under various land uses by employing the data of small indian experimental farms. In: Watershed management 2020. American Society of Civil Engineers, pp 141–150

Singh SK, Laari PB, Mustak SK, Srivastava PK, Szabó S (2018) Modelling of land use land cover change using earth observation data-sets of Tons River Basin, Madhya Pradesh, India. Geocarto Int 33(11):1202–1222

Singh S, Bhardwaj A, Verma VK (2020) Remote sensing and GIS based analysis of temporal land use/land cover and water quality changes in Harike wetland ecosystem, Punjab, India. J Environ Manag 262:110355

Singh G, Pandey A (2021) Evaluation of classification algorithms for land use land cover mapping in the snow-fed Alaknanda River Basin of the Northwest Himalayan Region. Appl Geomat. https://doi.org/10.1007/s12518-021-00401-3

Swain S, Dayal D, Pandey A, Mishra SK (2019a) Trend analysis of precipitation and temperature for Bilaspur District, Chhattisgarh, India. In: World Environmental and Water Resources Congress 2019: groundwater, sustainability, hydro-climate/climate change, and environmental engineering. American Society of Civil Engineers, pp 193–204

Swain S, Mishra SK, Pandey A (2019b) Spatiotemporal characterization of meteorological droughts and its linkage with environmental flow conditions. In: AGU fall meeting abstracts (AGUFM 2019), H13O–1959

Swain S, Mishra SK, Pandey A (2020a) Assessment of meteorological droughts over Hoshangabad district, India. In: IOP conference series: earth and environmental science, vol 491, p 012012. IOP Publishing

Swain S, Mishra SK, Pandey A (2021a) A detailed assessment of meteorological drought characteristics using simplified rainfall index over Narmada River Basin, India. Environ Earth Sci 80:221

Swain S, Mishra SK, Pandey A, Dayal D (2021b) Identification of meteorological extreme years over central division of odisha using an index-based approach. In: Hydrological extremes. Springer, Cham, pp 161–174

Swain S, Mishra SK, Pandey A (2021c) Assessing contributions of intensity-based rainfall classes to annual rainfall and wet days over Tehri Catchment, India. In: Advances in Water Resources and Transportation Engineering. Springer, Singapore, pp 113–121. https://doi.org/10.1007/978-981-16-1303-6_9

Swain S, Patel P, Nandi S (2017) Application of SPI, EDI and PNPI using MSWEP precipitation data over Marathwada, India. In: 2017 IEEE international geoscience and remote sensing symposium (IGARSS). IEEE, pp 5505–5507

Swain S, Sharma I, Mishra SK, Pandey A, Amrit K, Nikam V (2020b) A framework for managing irrigation water requirements under climatic uncertainties over Beed District, Maharashtra, India. In: World Environmental and Water Resources Congress 2020: water resources planning and management and irrigation and drainage. American Sociiety of Civil Engineers, pp 1–8

Swain S, Verma MK, Verma MK (2018) Streamflow estimation using SWAT model over Seonath river basin, Chhattisgarh, India. In: Hydrologic modeling. Springer, Singapore, pp 659–665

Talukdar S, Singha P, Mahato S, Pal S, Liou YA, Rahman A (2020) Land-use land-cover classification by machine learning classifiers for satellite observations—a review. Rem Sens 12(7):1135

Tian H, Banger K, Bo T, Dadhwal VK (2014) History of land use in India during 1880–2010: large-scale land transformations reconstructed from satellite data and historical archives. Global Planet Change 121:78–88

Tran DX, Pla F, Latorre-Carmona P, Myint SW, Caetano M, Kieu HV (2017) Characterizing the relationship between land use land cover change and land surface temperature. ISPRS J Photogramm Remote Sens 124:119–132

Tripathi G, Pandey AC, Parida BR, Kumar A (2020) Flood inundation mapping and impact assessment using multi-temporal optical and SAR satellite data: a case study of 2017 Flood in Darbhanga district, Bihar, India. Water Resour Manag 34(6):1871–1892